Entropic Contributions in Cosolvent Binding to Hydrophobic Solutes in Water

N. F. A. van der Vegt* and W. F. van Gunsteren

Laboratory of Physical Chemistry, Swiss Federal Institute of Technology Zürich, ETH-Hönggerberg, CH-8093 Zürich, Switzerland

Received: April 28, 2003; In Final Form: October 17, 2003

Gas solubility in liquids is driven by favorable solute−solvent interactions while being opposed by the entropic cost of creating a molecular-sized cavity of suitable size. We have investigated these contributions to the solvation free energy of small hydrophobic solutes and studied the dependence of the entropy cost of solute insertion on solvent−solvent interactions in cosolvent/water mixtures by means of molecular dynamics simulations. The cosolvents acetone, dimethyl sulfoxide, and sodium chloride were studied. Acetone, which weakly interacts with water relative to hydrogen-bonding interactions in neat water, preferentially binds to hydrophobic solutes thereby raising their solubility. We find that this process is driven by a reduced entropic expense of opening up molecular-sized cavities close to the acetone methyl moieties. Sodium chloride and dimethyl sulfoxide are strongly hydrated, causing entropy to oppose hydrophobic solute insertion even stronger than it does in neat water. In sodium chloride/water the solute is preferentially "wetted" causing it to be "salted-out". Dimethyl sulfoxide methyl moieties bind to the hydrophobic solute. This process, occurring at the expense of entropy, is driven by a favorable solute−solvent energy and causes "salting-in" of the hydrophobic solute.

1. Introduction

The thermodynamics of hydrophobic solvation in cosolvent/water mixtures governs the stability of biomolecular structures such as proteins and membranes.[1−5] In chemistry and biochemistry, "salting-in" and "salting-out" of solutes, driven by the addition of cosolvent species (e.g., salts, urea) to aqueous solutions, is a phenomenon usually exploited to steer self-organization and molecular recognition processes or to study the stability of peptides and proteins. The microscopic driving forces that control the solubility of nonpolar solutes and the thermodynamic stability of (bio)molecular structures are, however, still poorly understood as evidenced by ongoing discussion on the nature of hydrophobic effects.[6−10]

In this paper, we use molecular dynamics simulations to examine how the solubility of small nonpolar gas molecules in cosolvent/water mixtures can be understood from the nature of the molecular interactions in solution. As our liquid solvent consists of strongly associating (hydrogen-bonding) polar species (vide infra), the problem entails a detailed study of the role of the entropy rather than the energetics which would suffice to describe solvation in regular solutions.[11,12] Entropy changes are responsible for the hydrophobic effect defined here as the low solubility of nonpolar solutes in water compared to nonpolar organic solvents. The effect of solvent−solvent interactions (hydrogen bonding) on the solvation entropy of nonpolar solutes in water is, in fact, a topic of ongoing debate in the literature.[13−19] We, however, focus our attention on cosolvent/water mixtures. Motivated by the absence of a general atomic level picture of the effects of cosolvents on peptide and protein structure, our initial attempt focuses on the properties of simple nonpolar solutes. Some of the thermodynamic aspects of the action of cosolvents are well established. Salting-in of solutes is driven by preferential binding of the cosolvent to the solute, whereas salting-out is driven by a preferential exclusion of the cosolvent from the solute surface.[20−22] The microscopic driving forces responsible for this binding (exclusion) process, however, are less well understood and are subject of this study.

A detailed analysis of the solvation process has illustrated that the pertinent thermodynamic quantities determining solubility involve integrals over the potential energy of interactions between the solute and the solvent only.[23,24] The analysis showed that a change in the solvent−solvent energy due to structural reorganization of the solvent (i.e., the solvent reorganization energy) does not affect the solubility in any way. The solvent reorganization energy accounts for the formation of a cavity of correct size to accommodate the solute while having the solvent molecules in the equilibrium orientation appropriate for accommodating all chemical moieties of the solute. While the solvent reorganization energy contributes to both the solvation energy and the solvation entropy, both contributions exactly cancel in the solvation free energy. Yet, the solvent−solvent energy enters the solvation free energy indirectly through the canonical averages over solute−solvent terms.[23,24] In this sense, solvent−solvent interactions influence the solubility too but, as will become clearer later on, through a contribution measuring the entropic cost to insert the solute. This entropic penalty, which always opposes the solvation process, expresses an excluded volume effect that results from selecting solvent configurations possessing a cavity of suitable size and shape to accommodate the solute (i.e., the entropic cost to "lump small free volume packets") in the full statistical ensemble of the liquid solvent.[13,14,25]

Cavities are formed by breaking solvent−solvent contacts. In nonideal cosolvent/water mixtures differences in the strength of solvent−solvent interactions among the species of both kinds may have two implications. First, opening up a cavity may get

* Author to whom correspondence should be addressed. Current address: Max-Planck-Institute for Polymer Research, Ackermannweg 10, D-55128 Mainz, Germany. Phone: +49 6131 379 245. Fax: +49 6131 379 340. E-mail: vdervegt@mpip-mainz.mpg.de.

10.1021/jp030532c CCC: $27.50
Published on Web 12/19/2003

easier (or more difficult) than in neat water thereby lowering (or increasing) the entropic cost of solute insertion. Second, excess coordination of water/water (ww), cosolvent/cosolvent (cc), or cosolvent/water (cw) pairs may occur, a process which can be quantified by means of Kirkwood−Buff integrals, $G_{\alpha\beta}$, between solvent species α and β.[26,27] Thermodynamic nonidealities of the mixture, as revealed by a composition-dependent derivative of the cosolvent molar activity or mole fraction scale activity coefficient, appear in the case where $G_{cc} + G_{ww} - 2G_{cw} \neq 0$.[27−29] Such nonidealities may cause cavities to be preferentially solvated by either water or the cosolvent depending on the relative ease of cavity formation in spatial regions of fluctuating solvent composition. Some salting-in or salting-out effects due to differences of cc, ww, and cw interactions are well understood. For example, when a strong electrolyte is chosen as a "cosolvent", cw interactions lead to salt ion hydration. Small ions of high charge density (kosmotropes or structure makers) bind water molecules strongly, whereas large monovalent ions of low charge density (chaotropes or structure breakers) bind water molecules weakly relative to the strength of water−water interactions in bulk solution.[30] As a result, kosmotropes interact unfavorably with hydrophobic solutes in water, whereas chaotropes associate favorably with hydrophobic solutes. Computer simulation studies have shown that cavities are unlikely to open up in the hydration shell of small strongly hydrated ions (alkali halides) causing the salt to be excluded from the cavity surface while causing an increase of the local water density near the cavity surface (preferential hydration).[6,31] Because the interactions between the hydration waters and the ion are stronger than those between the water molecules themselves, the flexibility of the medium to open up a cavity is reduced (relative to neat water) and the nonpolar solute is salted out. This effect is entropic in nature.

In this paper we discuss the role of entropy in the molecular dissolution process of methane in binary mixtures of water with sodium chloride, dimethyl sulfoxide, and acetone. Acetone/water is known to show strong excess water−water aggregation;[29] hence, acetone−water interactions are expected to be weak compared to water−water interactions. Addition of acetone to water may therefore facilitate cavity formation in "acetone-rich pools", causing an entropy-driven salting-in of nonpolar solutes. In DMSO/water mixtures, on the other hand, experimental studies showed no strong solvation of a molecule by molecules of the same species or the other component.[32] We have studied these systems by means of molecular dynamics simulation over all possible composition ranges. The NaCl/water system was studied at salt concentrations of up to 6 M. The DMSO/water and acetone/water systems were studied at various compositions ranging between the limits of pure water and pure liquid cosolvent. We will show that in the NaCl/water and acetone/water systems, changes of the methane solubility with mixture composition are governed by entropy changes while in the DMSO/water system a balance of solute−solvent energy and entropy determine methane solubility changes. The change in methane solubility with solvent composition is discussed in terms of preferential cosolvent binding to (or repulsion from) the nonpolar solute surface and the intermolecular solvent interactions in the liquid mixture.

2. Theory

2.1. Solvation Gibbs Energy. Solvation, as suggested by Ben-Naim, refers to the transfer of a solute molecule (S) from a fixed position in the ideal gas phase to a fixed position in the solvent at constant temperature and pressure.[33] The solute−solvent (binding) interaction, B_s, established by inserting a test-particle S at some random point in an N-particle liquid configuration is the difference of the $N + 1$ and N particle potential energies, $B_S = U_{N+1} - U_N$. On the basis of Widom's potential distribution theorem,[34] the Ben-Naim standard Gibbs energy change is

$$\Delta G_S^* = -RT \ln[\langle V \exp(-B_S/RT)\rangle_{NPT}/\langle V\rangle_{NPT}] \qquad (1)$$

where the ensemble average is taken over pure solvent configurations at constant pressure P and temperature T. In eq 1, V denotes the system volume and $\langle V\rangle_{NPT}$ its constant pressure−temperature ensemble average. The test particles invoked to compute ΔG_S^* are never really inserted but merely act as probes that do not affect the solvent trajectory.

2.2. Solvation Enthalpy and Entropy. The solvation entropy and enthalpy are important complements to the solvation free energy because they provide additional information that helps one to understand and interpret the connection between changes in the molecular nature of the solute−solvent interactions and the changes in the thermodynamic properties. For example, a solute may have similar solvation Gibbs energies in different solvents even though its solubility is determined by very different phenomena at the molecular level. The solubility in solvent A could be driven by a favorable enthalpy while the solvation process causes a loss of entropy, whereas in solvent B the solubility could mostly be driven by a favorable entropy with very little energy change.

The enthalpy change associated with the solute solvation process is

$$\Delta H_S^* = \Delta U_S^* + P\Delta V_S^* \qquad (2)$$

where ΔU_S^* and ΔV_S^* are the energy change and volume change, respectively. In eq 2, the $P\Delta V_S^*$ term is typically two orders of magnitude smaller than ΔU_S^*; therefore, it will be neglected below.

The total potential energy of the solution can be subdivided in a solute−solvent term, U_{uv}, and a solvent−solvent term, U_{vv}, defined as the interaction energy of the solute with the solvent and the sum of interaction energies of the solvent molecules with all other solvent molecules, respectively. On the basis of this subdivision, the solvation energy is expressed as

$$\Delta U_S^* = \Delta U_{uv}^* + \Delta U_{vv}^* \qquad (3)$$

where ΔU_{uv}^* is the solute binding energy to the solvent and ΔU_{vv}^* is the solvent reorganization energy associated with the introduction of the solute at some fixed position in the liquid. In terms of the notation introduced in Section 2.1 we write

$$\begin{aligned}\Delta U_S^* &= \langle U_{N+1}\rangle_{N+1PT} - \langle U_N\rangle_{NPT} \\ &= \langle U_N + B_S\rangle_{N+1PT} - \langle U_N\rangle_{NPT} \\ &= \langle B_S\rangle_{N+1PT} + [\langle U_N\rangle_{N+1PT} - \langle U_N\rangle_{NPT}]\end{aligned} \qquad (4)$$

where $\langle\cdots\rangle_{N+1PT}$ is the $N + 1$ particle ensemble (the solution) average and $\langle\cdots\rangle_{NPT}$ is the N particle ensemble (the solvent) average. Hence,

$$\Delta U_{uv}^* = \langle B_S\rangle_{N+1PT} \quad \text{and} \quad \Delta U_{vv}^* = \langle U_N\rangle_{N+1PT} - \langle U_N\rangle_{NPT} \qquad (5)$$

These energies can be expressed in a form involving averaging

over configurations of the N particle (neat solvent) system only. Using

$$\langle \Psi \rangle_{N+1PT} = \frac{\langle \Psi V \, e^{-B_S/RT} \rangle_{NPT}}{\langle V \, e^{-B_S/RT} \rangle_{NPT}} \tag{6}$$

where Ψ is a function of the configurational space coordinates, the test-particle equations for the solute−solvent and solvent−solvent energy read

$$\Delta U^*_{uv} = \frac{\langle B_S V \, e^{-B_S/RT} \rangle_{NPT}}{\langle V \, e^{-B_S/RT} \rangle_{NPT}} \tag{7}$$

$$\Delta U^*_{vv} = \frac{\langle \delta U_N V \, e^{-B_S/RT} \rangle_{NPT}}{\langle V \, e^{-B_S/RT} \rangle_{NPT}} \tag{8}$$

In eq 8, $\delta U_N = U_N - \langle U_N \rangle_{NPT}$ is the instantaneous fluctuation of the solvent−solvent interaction energy.

It is noteworthy that the solvent reorganization energy affects values of enthalpy and entropy significantly, even changing their signs, but it does not affect the solubility in any way as it does not appear explicitly in eq 1.[23,24] The energy change due to solvent reorganization is exactly counterbalanced by a term in the solvation entropy which causes it to cancel in the solvation Gibbs energy. To illustrate the cancellation of ΔU^*_{vv}, the solvation energy and entropy is written as[24,35]

$$\begin{aligned} \Delta U^*_S &= \Delta U^*_{uv} + \Delta U^*_{vv} \\ \Delta S^*_S &= \Delta S^*_{uv} + (\Delta U^*_{vv}/T) \end{aligned} \tag{9}$$

to yield the solvation Gibbs energy

$$\Delta G^*_S = \Delta U^*_{uv} - T\Delta S^*_{uv} \tag{10}$$

which then contains energetic and entropic terms both of which are functions of only the solute−solvent interaction, with the solvent−solvent interactions occurring implicitly in the ensemble averaging.[23] In eq 10, ΔU^*_{uv} is the solute binding energy introduced above and ΔS^*_{uv} is a fluctuation term (the *solute−solvent entropy*), defined by eq 9, that expresses the entropic cost to insert the solute. In the hypothetical case of a purely repulsive solute, ΔU^*_{uv} is positive or zero (i.e., for a hard sphere) and the entropic term ΔS^*_{uv} is negative, both opposing the dissolution process. For real solutes, ΔU^*_{uv} and ΔS^*_{uv} are both negative, the former favoring the dissolution process while the latter opposes it.

There are two features that are important in determining the entropy change that accompanies the dissolution process (see eq 9). First, the solvation process requires the formation of a cavity which is of the correct size to accommodate the solute. This cavity has the solvent molecules in the equilibrium orientation appropriate for accommodating all chemical moieties of the solute. Because the solvent is excluded from the volume taken by the cavity, this part of the solvation process causes a reduction of the entropy, the magnitude of which is given by the ΔS^*_{uv} term in eq 9. Second, formation of the above cavity affects the local binding energy among solvent molecules near the cavity over its corresponding value in the bulk. Looser binding (i.e., a positive ΔU^*_{vv}) between solvent molecules in the solvation shell compared with the binding in the bulk solvent causes an increased configurational freedom and thus an increase of the entropy, the magnitude of which is given by the $\Delta U^*_{vv}/T$ term in eq 9. Correspondingly, tighter binding (i.e., a negative ΔU^*_{vv}) reduces the configurational freedom of the solvation shell thereby reducing its entropy. We note that, at constant pressure, the solvent reorganization energy, ΔU^*_{vv}, can be traced back to perturbations of the solution structure near the solute.[35] Under this condition, nonlocal contributions to ΔU^*_{vv}, due to a bulk solvent response, are absent (at constant volume conditions this is no longer valid and nonlocal contributions to ΔU^*_{vv} arise).[35]

The phenomenon of perfect entropy−enthalpy compensation as expressed by eqs 9 and 10 is a thermodynamic requirement. Therefore, it is independent of interaction potential functions and conveys no specific information on molecular interactions. The solute−solvent energy and entropy generally show strong compensation behavior too, as both quantities carry negative signs. This type of (partial) energy−entropy compensation depends on molecular interactions and the solute's size and shape. An increase of solute size often (but not always) causes a stronger negative value of both ΔU^*_{uv} and ΔS^*_{uv}. This compensation behavior, which is not required by thermodynamic laws, is currently not well understood.[36,37]

2.3. Pair Distribution Functions and Preferential Solvation. Pair distribution functions may be used to describe solute−solvent correlations and are calculated here in order to examine preferential solvation processes in cosolvent/water mixtures. Since all thermodynamic properties above can be obtained through the Widom particle-insertion technique from a single molecular dynamics (MD) run of the neat solvent, the most elegant way to obtain the pair correlation functions is from the same simulation as well. Let $\Psi(\mathbf{r})$ be a quantity such as $(1/N)[\sum_{i=1}^{N} \delta(\mathbf{r}_{si} - \mathbf{r})]$, where δ is the Dirac delta function and $\mathbf{r}_{si}$ designates the location of the ith solvent particle with respect to the atomic solute. Then eq 6 is the test-particle expression for a pair distribution function. We compute solute−water and solute−cosolvent pair correlation functions to investigate the local solvent composition in the vicinity of solutes. Moreover, the solvent structure in the proximity of empty cavities is studied. The formation of an empty cavity is determined by the properties of the solvent only. Its solvation structure shows where (close to which atomic groups) density fluctuations in the solvent most favor the appearance of a cavity. The latter information points out the entropically favored solute location while the former is affected by the nature of solute−solvent interactions too.

On the basis of the Kirkwood−Buff (KB) theory of solution,[26,27] the local solvent composition above can be related to the derivative, $(\partial \Delta G^*_S/\partial x_C)_{PT}$, of the solute solvation Gibbs energy with the cosolvent mole fraction (x_C) of the binary solvent. If ρ_S, ρ_C, and ρ_W denote, respectively, the solute, cosolvent, and the water number density of the solution, KB theory derives[27]

$$\lim_{\rho_S \to 0} \left(\frac{\partial \Delta G^*_S}{\partial x_C} \right)_{PT} = \frac{RT(\rho_W + \rho_C)^2}{\eta} (G_{WS} - G_{CS}) \tag{11}$$

where η is a positive constant, and G_{WS} and G_{CS} are the solute−water and solute−cosolvent KB integrals defined by

$$G_{\alpha S} = \int_0^\infty [g_{\alpha S}(R) - 1] 4\pi R^2 \, dR \tag{12}$$

In eq 12, $g_{\alpha S}(R)$ is the radial distribution function for the pair of species α and S. $\rho_\alpha G_{\alpha S}$ is the excess coordination number measuring the excess of component α in the correlation

TABLE 1: Nonbonded Interaction Parameters[a]

	$C_{12}^{1/2}(i,i)$ 10^{-3} (kJ/mol nm^{12})$^{1/2}$	$C_6^{1/2}(i,i)$ (kJ/mol nm^6)$^{1/2}$	σ_i (nm)	ϵ_i (kJ/mol)	q_i (e)
C (carbonyl)	1.653 19	0.043 582	0.3360	0.3300	0.565
O (carbonyl)	1.328 29	0.044 587	0.3100	0.5600	−0.565
S (sulfoxide)	4.636 60	0.102 770	0.3560	1.2972	0.139
O (sulfoxide)	0.866 86 (1.125)[b]	0.047 652	0.2630 (0.2869)[b]	1.7154 (1.0180)[b]	−0.459
CH_3	5.162	0.098 05	0.3748	0.8672	0.16 (DMSO) 0.00 (acetone)
O (water)	1.623	0.051 16	0.3166	0.6502	−0.82 (SPC) −0.8476 (SPC/E)
H (water)	0.00	0.00	0.00	0.00	0.41 (SPC) 0.4238 (SPC/E)
Na^+	0.1450	0.008 489	0.2575	0.0617	1.00
Cl^-	10.340	0.117 5	0.4448	0.4457	−1.00
Ar	3.086 05	0.078 52	0.3400	0.9977	0.00
Kr	5.191 07	0.111 26	0.3600	1.4218	0.00
CH_4	6.042 85	0.116 16	0.3733	1.2466	0.00

[a] The nonbonded interaction function is given by the following:

$$V(r_{ij}) = \frac{C_{12}(i,j)}{r_{ij}^{12}} - \frac{C_6(i,j)}{r_{ij}^{6}} + \frac{q_i q_j}{4\pi\epsilon_0}\left[\frac{1}{r_{ij}} + \frac{(\epsilon_{RF}-1)r_{ij}^{2}}{(2\epsilon_{RF}+1)R_C^{3}} - \frac{3\epsilon_{RF}}{(2\epsilon_{RF}+1)R_C}\right]$$

where R_C is the long-range cutoff radius, $C_{12}(i,i) = 4\epsilon_i\sigma_i^{12}$, $C_6(i,i) = 4\epsilon_i\sigma_i^6$ and σ_i and ϵ_i are the Lennard-Jones size and well depth, respectively. The combination rules are given by the following: $C_6(i,j) = C_6(i,i)^{1/2}C_6(j,j)^{1/2}$; $C_{12}(i,j) = C_{12}(i,i)^{1/2}C_{12}(j,j)^{1/2}$. [b] The value in parentheses is used for the interaction with the water oxygen.

volume[27] of the solute. Since $\eta > 0$, the quantity $RT(\rho_W + \rho_C)^2/\eta$ is always positive and the sign of the derivative in eq 11 is the same as the sign of $(G_{WS} - G_{CS})$. Thus, eq 11 expresses the intuitive notion that preferential cosolvent binding to the solute promotes the solubility of the latter. Because eq 11 can be used to describe changes of the solvation Gibbs energy, $\Delta\Delta G_S^*$, relative to solvation in pure water as well, it can, for example, be applied to peptides and proteins too.[27] We emphasize that no assumptions have been made in its derivation.

Changes in the entropy costs of opening up molecular-sized cavities in cosolvent/water mixtures can also be rationalized using KB theory. If one defines a cavity as a spherical region in the fluid from which the centers of all solvent molecules are excluded, the cavity formation work, ΔG_{cav}^*, is identical to the solvation Gibbs energy ΔG_{HS}^* of a hard sphere (HS) of the appropriate size.[27] Because the solvent reorganization energy associated with the formation of this cavity is exactly compensated by an identical term in the entropy, ΔG_{cav}^* is purely entropic and is given by $\Delta G_{cav}^* = -T\Delta S_{HS}^*$ (i.e., eq 10 with $\Delta U_{uv}^* = 0$).[13,14,25] Application of eq 11 to the solvation process of a hard sphere yields

$$\lim_{\rho_{HS}\to 0}\left(\frac{\partial T\Delta S_{HS}^*}{\partial x_C}\right)_{PT} \sim (G_{C,HS} - G_{W,HS}) \qquad (13)$$

This relation states that opening up a cavity in a cosolvent/water mixture becomes entropically cheaper as a result of addition of cosolvent if the cosolvent preferentially binds to the cavity. Cavities will readily open up close to the cosolvent if the cosolvent−water interactions are weaker than the water−water interactions. Opening of cavities in the solvation shell of the cosolvent is inhibited when the cosolvent−water interactions are stronger than the bulk water−water interactions. An example of the latter is provided by kosmotropic ions.

3. Methods

Simulations of water and mixtures of NaCl/water, acetone/water, and DMSO/water were carried out using the GROMOS96 biomolecular simulation package.[38] The acetone model of Weerasinghe and Smith[29] was used in all acetone/water simulations. For DMSO, we used a preliminary version of the model recently parametrized by Geerke et al.[39] in which the geometry and the atomic charges are still those of GROMOS96.[38] The parameters for the methyl groups were taken from a recent reparametrization of the GROMOS96 aliphatic hydrocarbons.[40] The GROMOS96 force field was used to describe all bonded terms. Sodium chloride and acetone/water mixtures were simulated with the SPC/E water model.[41] For DMSO/water mixtures, the SPC water model[42] was used. The nonbonded interaction parameters have been summarized in Table 1, together with the parameters for the nonpolar solutes. All system compositions studied have been specified in Table 2. Before collecting the trajectories, all systems were allowed to equilibrate for at least 1 ns. A twin-range cutoff scheme with 0.8 and 1.4 nm cutoff radii was applied. The nonbonded interactions in the range between these radii were updated every fifth time step. A time step of 2 fs was used. A reaction field approximation was used to account for truncation of electrostatic forces beyond the long-range cutoff (1.4 nm). The reaction field relative dielectric permittivities, ϵ_{RF}, are listed in Table 2. Constant pressure (1 atm) and temperature (298 K) simulations were performed using a weak coupling scheme with relaxation times of 0.1 ps (temperature) and 0.5 ps (pressure).[43] The solute and solvent degrees of freedom were coupled to a single heat bath (acetone/water and DMSO/water) or to separate baths (NaCl/water). All bond lengths were kept constant using the SHAKE algorithm[44] using a relative geometrical tolerance of 10^{-4}. Solvation free energies and solute−solvent energies and entropies were obtained by performing at least 2.5×10^8 test-particle insertions in 1−2 ns simulation trajectories. The insertion points were chosen at random. The statistical accuracy of this combination of run times and number of test insertions was analyzed by a block-averaging procedure. The statistical uncertainties in the solvation free energies and solute−solvent energies and entropies were found to be less than 0.2 kJ/mol.

4. Results

4.1. Neat Water. Table 3 shows the thermodynamic hydration quantities of argon, krypton, and methane in simple point charge

TABLE 2: Summary of the MD Simulations of Cosolvent/Water Mixtures[a]

N_C	N_{H_2O}	x_C	ρ_C (M)	t_{MD} (ns)	ϵ_{RF}	T (K)	V (nm^3)	ρ (g/cm^3)
				Water (SPC)				
0	739	0.0	0.0	21.0	54	302.3	22.73	0.973
				Water (SPC/E)				
0	739	0.0	0.0	1.0	54	302.6	22.22	0.994
				NaCl/Water (SPC/E)				
8	1000	0.008	0.44	1.6	54	302.9	30.22	1.016
16	1000	0.016	0.87	1.6	54	302.9	30.43	1.034
32	1000	0.031	1.72	1.6	54	303.0	30.94	1.067
64	1000	0.060	3.26	1.6	54	302.7	32.57	1.109
125	1000	0.111	5.80	1.6	54	302.2	35.80	1.174
				Acetone/Water (SPC/E)				
168	1512	0.10	4.36	1.0	50	299.3	63.93	0.961
275	1100	0.20	7.14	1.0	39	298.4	63.96	0.929
396	594	0.40	10.36	1.0	25	297.7	63.49	0.881
432	432	0.50	11.32	1.0	28	297.5	63.36	0.862
462	308	0.60	12.07	1.0	23	297.4	63.54	0.846
500	125	0.80	13.06	1.0	18	297.4	63.55	0.818
513	57	0.90	13.43	1.0	16	297.3	63.42	0.807
520	0	1.00	13.71	1.0	15	297.3	62.97	0.796
				DMSO/Water (SPC)				
43	812	0.05	2.37	1.3	77.4	299.7	30.14	0.991
91	812	0.10	4.22	1.3	75.7	299.2	35.78	1.009
188	812	0.19	6.63	1.2	72.4	298.7	47.08	1.034
241	651	0.27	8.30	1.3	70.1	298.5	48.22	1.052
349	651	0.35	9.54	2.2	67.2	298.3	60.75	1.066
478	522	0.48	11.05	2.2	63.0	298.3	71.83	1.081
331	186	0.64	12.37	2.3	57.9	298.2	44.43	1.092
814	186	0.81	13.31	2.1	52.0	298.3	101.54	1.095
512	0	1.00	14.00	2.2	46.0	298.5	60.73	1.094

[a] N_C is the number of cosolvent molecules, N_{H_2O} is the number of water molecules, x_C is the cosolvent mole fraction, ρ_C is the cosolvent molarity, t_{MD} is the simulation run time, ϵ_{RF} is the reaction field relative dielectric permittivity, T is the average temperature of the simulation, V is the average volume of the simulation, and ρ is the density.

TABLE 3: Thermodynamic Quantities of Nonpolar Gas Hydration in SPC and SPC/E Water at 302 K and 1 Atm[a]

nonpolar gas	ΔG^*_S	$-\Delta H^*_S$	$-T\Delta S^*_S$	$-\Delta U^*_{uv}$	ΔU^*_{vv}
			SPC Water		
Ar	8.5 (8.4)	7.7 (7.4)	16.2 (15.9)	10.2	2.5
Kr	7.2 (7.1)	11.1 (10.9)	18.3 (18.0)	14.0	2.9
CH_4	8.7 (8.4)	10.2 (9.2)	18.9 (17.6)	13.5	3.3
			SPC/E Water		
Ar	8.9 (8.4)			10.5	
Kr	7.7 (7.1)			14.4	
CH_4	9.3 (8.4)			13.9	

[a] ΔG^*_S is the solvation Gibbs energy, ΔH^*_S is the solvation enthalpy, ΔS^*_S is the solvation entropy, ΔU^*_{uv} is the solute−solvent energy, and ΔU^*_{vv} is the solvent−solvent energy (solvent reorganization energy). The units are kJ/mol. The solvation enthalpy was calculated from eqs 2 and 3 with the $P\Delta V^*_S$ term ignored. Experimental values, taken from ref 45, are shown in parentheses.

(SPC) water at 1 atm and 302 K. For comparison, the solvation Gibbs energies and solute−solvent energies in SPC/E water are shown as well. To obtain a statistically converged solvent−solvent energy change, 1.625×10^9 test-particle insertions were performed during a 21 ns MD run. The experimentally determined data, shown within parentheses, are well reproduced. In all cases, the entropic terms are larger in absolute value than the enthalpic terms resulting in unfavorable hydration free energies. This behavior is typical of hydrophobic hydration. In general, the solute−solvent energies are large and negative, exceeding the solvent reorganization energies in absolute value. The latter contribute up to 30% to the total hydration enthalpies and therefore must be taken into consideration in order to achieve satisfactory agreement with experiment. The solvent reorganization energies are small compared to their corresponding values in organic liquids because of water's attempt to reorganize without sacrificing hydrogen bonds. Because ΔU^*_{vv} is a compensating term in the Gibbs energy change, it has no effect on the solubility. The only contributions that determine solubility are the solute−solvent terms to which we will limit our attention below.

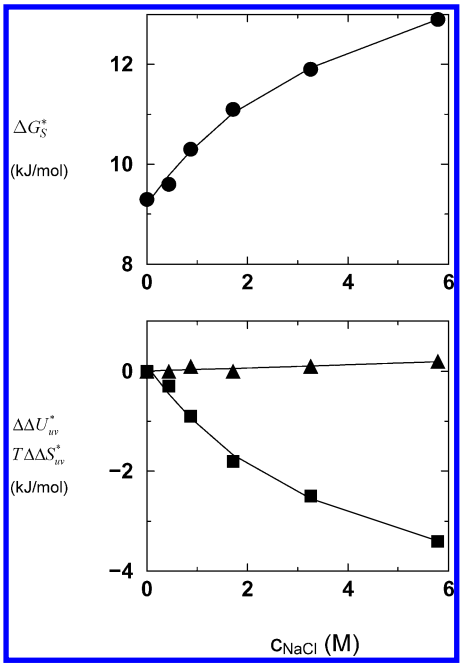

Figure 1. Methane solvation Gibbs energy (upper panel) and solute−solvent energy $\Delta\Delta U^*_{uv}$ (triangles) and entropy $T\Delta\Delta S^*_{uv}$ (squares) relative to neat water (lower panel) vs the salt concentration of the solution.

We note that the energies presented in Table 3 were calculated at constant pressure. Under this condition $(\Delta H^*_S)_P \approx (\Delta U^*_S)_P$ because the $P\Delta V^*_S$ term is usually small.[33] Unlike the solvation free energy, solvation enthalpies and entropies are ensemble dependent. Differences between the solvation enthalpy $(\Delta H^*_S)_P$ (at constant pressure) and the solvation energy $(\Delta U^*_S)_V$ (at constant volume) are, however, usually large and, in the thermodynamic limit, are given by $(\Delta H^*_S)_P - (\Delta U^*_S)_V = \Delta V^*_S T\alpha/\kappa$.[35] Here, α denotes the thermal expansion coefficient and κ denotes the compressibility of the solvent.

4.2. Sodium Chloride/Water. Figure 1 shows the methane solvation Gibbs energy (upper panel) and the corresponding solute−solvent energy and entropy changes (lower panel) as a function of sodium chloride concentration in water. The latter quantities are both presented relative to the value in neat water. The propensity of NaCl to salt out methane is evident from the rise of ΔG^*_S, which results from a reduction of the solute−solvent entropy. The solute−solvent energy change is hardly affected by the addition of NaCl. At all salt concentrations $|\Delta\Delta U^*_{uv}| < 0.2$ kJ/mol. The positive slope of ΔG^*_S indicates that methane is preferentially hydrated (Section 2.3).

In Figure 2 we present the difference, $\delta_{\alpha,S}(R) = x_{\alpha,S}(R) - x_\alpha$, between the local mole fraction $x_{\alpha,S}(R)$ of solvent species α in a spherical region of radius R having the solute centered at the origin and the bulk mole fraction x_α. Also shown are the methane−water and methane−salt pair correlation functions. The first peak of the methane−sodium radial distribution function, $g(r)$, is weak and well outside of the methane−sodium Lennard-Jones interaction minimum (0.31 nm), whereas the peak of the methane−chloride $g(r)$ coincides with the methane−

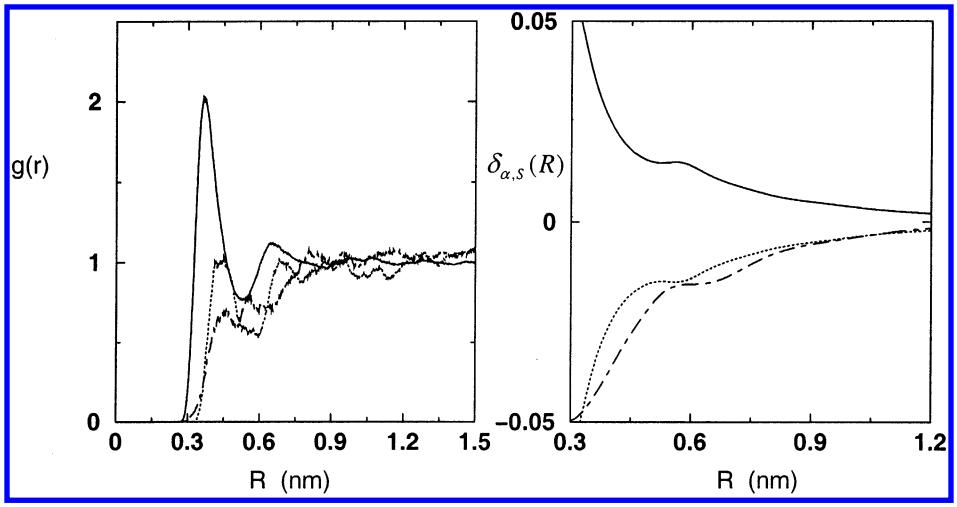

Figure 2. Methane−solvent radial distribution functions, $g(r)$, (left) and excess mole fractions, $\delta_{\alpha,S}(R)$, of solvent moieties α at distance R from the methane solute (right) for solvent moieties water (solid line), chloride (dotted line), and sodium (dot−dashed line). The bulk salt concentration is 3.3 M ($x_c = 0.06$).

chloride Lennard-Jones interaction minimum (0.41 nm). Hence, methane weakly associates with the Cl^- ion, while the methane−Na^+ solvent-mediated interaction is strongly repulsive. This observation agrees with previous work discussing hard sphere solutes in aqueous solutions of sodium chloride.[6] The behavior of $\delta_{\alpha,S}(R)$ indicates that methane is strongly hydrated at short distances while with increasing R water gets gradually replaced by salt (for $R \to \infty$, $\delta_{\alpha,S}(R) \to 0$). Integration over the first peak of the solute−water radial distribution function (up to $R = 0.525$ nm) gives 18 hydration waters (compared to 19 in neat water), 0.5 sodium ions, and 0.7 chloride ions. Positive nonzero values of $\delta_{W,S}$ (preferential hydration) are also observed at a larger distance R_C, where indirect correlations are included and all pair correlation functions have approached unity (at about $R_C = 1$ nm). In fact, this observation must hold thermodynamically because of the positive slope of the methane solvation Gibbs energy ΔG_S^* with sodium chloride concentration x_C shown in Figure 1. If $(\partial \Delta G_S^*/\partial x_C)_{PT} > 0$, eq 11 requires $G_{WS} - G_{CS} > 0$. With[27]

$$\delta_{W,S}(R_C) = \frac{x_W x_C (G_{WS} - G_{CS})}{x_W G_{WS} + x_C G_{CS} + V_{cor}} \qquad V_{cor} = {}^4/_3 \pi R_C{}^3 \quad (14)$$

the preferential hydration of the solute $\delta_{W,S}(R_C) > 0$, given that the denominator in eq 14 is always positive.

Because methane is preferentially hydrated, ΔU_{uv}^* values are hardly affected by the addition of salt. As the salt ions strongly bind water molecules, the spontaneous opening up of cavities in the solution becomes less probable upon addition of salt, resulting in a reduction of the solute−solvent entropy. This observation is in agreement with an information theory based analysis that showed that a larger free energy of cavity formation and a lower solubility in salt solutions can be attributed to reduced molecular density fluctuations.[6]

4.3. Acetone/Water. The acetone model studied in this work was developed by Weerasinghe and Smith.[29] It features average acetone−water pair interaction energies that are weaker than water−water pair interaction energies. The model, parametrized in combination with the SPC/E water model, exhibits water self-aggregation in agreement with experiment.[32] Compared to the NaCl/water system, the nature of the solvent−solvent molecular interactions in the acetone/water system prompts the supposition that molecular-sized cavities will more readily open up (relative to neat water) and will occur in the acetone solvation shell. If this picture holds, a positive change in the solute−solvent entropy upon addition of the cosolvent acetone to water acts as a microscopic driving force favoring the solubility of the solute.

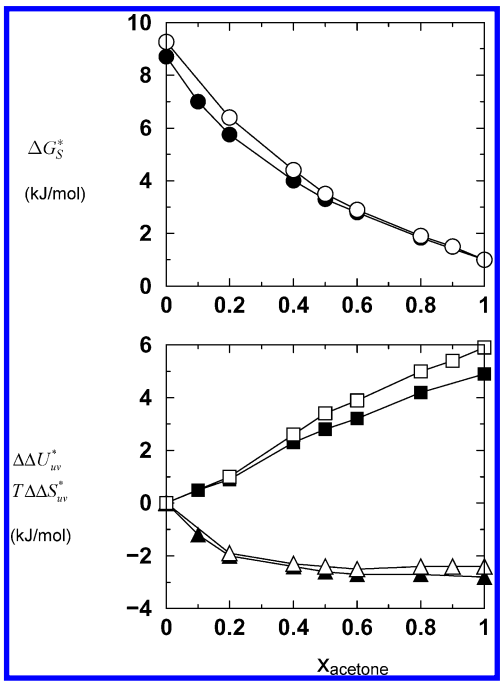

Figure 3. Methane solvation Gibbs energy (upper panel) and solute−solvent energy $\Delta\Delta U_{uv}^*$ (triangles) and entropy $T\Delta\Delta S_{uv}^*$ (squares) relative to neat water (lower panel) vs the acetone mole fraction of the solution. Solvent mixtures with SPC water (closed symbols) and SPC/E water (open symbols) are shown.

Figure 3 shows the methane solvation Gibbs energy (upper panel) and the corresponding solute−solvent energy and entropy changes (lower panel) as a function of the acetone mole fraction. Acetone strongly "salts in" the methane which is largely due to a significant increase of the solute−solvent entropy. The solute−solvent energy drops by about 2−3 kJ/mol relative to neat water; hence, the solute−solvent energy *and* entropy add constructively to produce a large favorable free energy change. Figure 3 shows the results obtained by combining the acetone model of Weerasinghe and Smith[29] with both the SPC/E (open symbols) and SPC (filled symbols) water models. The choice of water model does not significantly affect the solvation quantities.

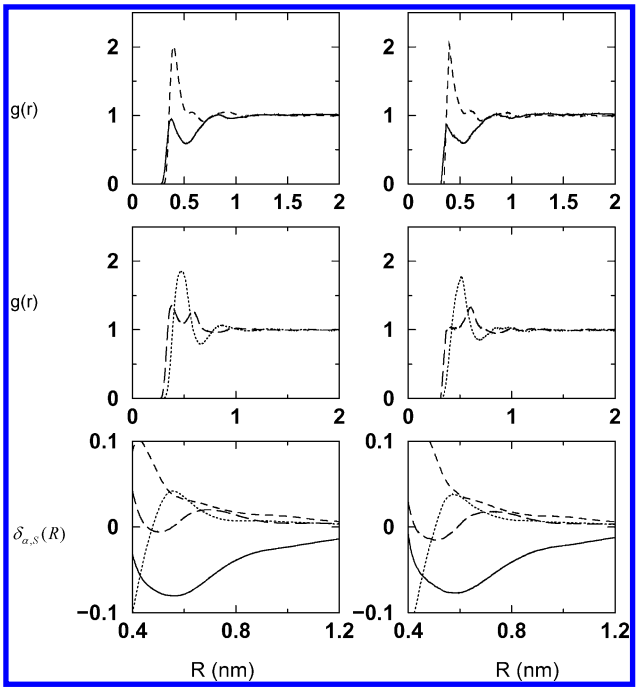

Figure 4. Methane−solvent radial distribution functions, $g(r)$, (upper two panels, left) and excess mole fractions, $\delta_{\alpha,S}(R)$, of solvent moieties α at distance R from the methane solute (lower panel, left) for solvent moieties water (solid line), methyl (dashed line), carbonyl carbon (dotted line), and carbonyl oxygen (long dashed line) at an acetone mole fraction of 0.5. The panels on the right show similar quantities for the cavity−solvent system.

Figure 4 presents methane−water and methane−acetone radial distribution functions (two upper left panels), as well as preferential solvation functions, $\delta_{\alpha,S}$ (lower left panel), at an acetone mole fraction of 0.5. In addition, these quantities are presented for empty methane-sized cavities (obtained by performing HS test-particle insertions) in the right panels. As expected from eq 11, acetone preferentially binds to methane. From the first maxima in the methane−acetone radial distribution functions as well as the behavior of the $\delta_{\alpha,S}$ curves for the methyl, carbonyl carbon, and carbonyl oxygen moieties, it appears that methane associates with the methyl and oxygen groups (with a strong preference for the former) of acetone. The shoulder in the flank of the CH_4-CH_3 peak (dashed line, upper left panel) is due to the second methyl group of acetone. The bifurcation of the CH_4−O(carbonyl) peak (long-dashed line, middle left panel) reveals that methane association with the oxygen competes with the oxygen's ability to hydrogen bond to water. This bifurcation partly disappears in the cavity−O(carbonyl) radial distribution function (long-dashed line, middle right panel), indicating that hydrogen bonding of the carbonyl oxygen to water prevails in this case. Integration over the first peak of the methane−water and methane−carbon (carbonyl) radial distribution functions (up to $R = 0.65$ nm) gives 4.9 hydration waters and 7.7 acetones. Figure 4 (lower right panel) shows that empty (methane-sized) cavities are preferentially solvated by acetone ($\delta_{C,HS}(R_C) > 0$). Cavity formation, therefore, becomes entropically less expensive by addition of acetone (cf. eq 13).

4.4. Dimethyl Sulfoxide/Water. In binary solutions water and DMSO strongly interact, and they are miscible in all proportions at room temperature.[46] DMSO−water interactions are stronger than acetone−water interactions because of a stronger hydrogen bond acceptor capacity of the DMSO oxygen. In our DMSO and acetone models this behavior is reflected by the larger DMSO molecular dipole moment (4.6 D for DMSO vs 3.3 D for acetone) and the smaller van der Waals (C_{12}) repulsion between the DMSO oxygen and the water oxygen (Table 1). Strong DMSO−DMSO interactions and DMSO−water interactions occur, respectively, in pure liquid DMSO and its mixtures with water. The DMSO heat of vaporization at $T = 298$ K and $P = 1$ atm amounts to 52.9 kJ/mol (compared to 44.0 kJ/mol for water), while the mixing enthalpy amounts to −3 kJ/mol in a 40/60 molar composition DMSO/water mixture.[39] At the same composition, the acetone−water mixing enthalpy amounts approximately to −0.4 kJ/mol.[29] The DMSO model used here was recently parametrized by Geerke et al.[39] and reproduces these features. It is worth noting that a KB analysis, based on experimental data, revealed neither a significant change of structural correlations with respect to the pure components nor any strong solvation of a molecule by molecules of the same species or the other component.[32] From this point of view, DMSO/water mixtures behave like an ideal liquid mixture, unlike acetone/water mixtures.

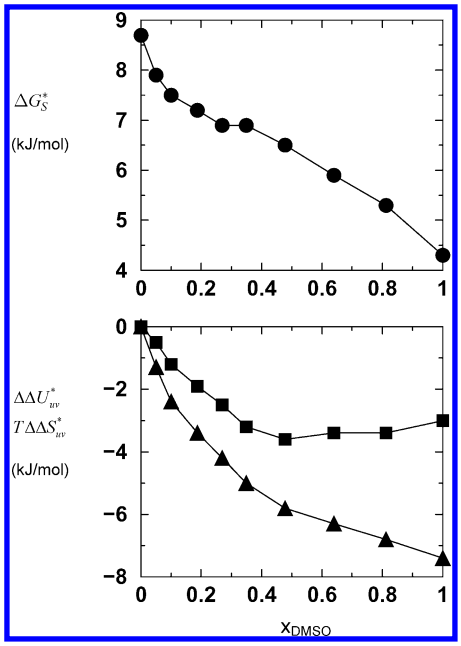

Figure 5. Methane solvation Gibbs energy (upper panel) and solute−solvent energy $\Delta\Delta U_{uv}^*$ (triangles) and entropy $T\Delta\Delta S_{uv}^*$ (squares) relative to neat water (lower panel) vs the DMSO mole fraction of the solution.

Figure 5 shows the methane solvation Gibbs energy (upper panel) and the corresponding solute−solvent energy and entropy changes (lower panel) as a function of the DMSO mole fraction. The addition of DMSO promotes the solubility of methane due to a favorable change in the solute−solvent energy. The solute−solvent entropy, however, opposes the preferential binding of DMSO to CH_4 up to a DMSO mole fraction of approximately 0.5 after which it appears to increase slightly upon further addition of DMSO. The solvent structure near methane and near the corresponding empty cavity are shown in Figure 6 for a DMSO mole fraction of 0.48. At this composition, the solvation Gibbs energy change with x_{DMSO} has a negative slope while that of the solute−solvent entropy vanishes. The statistical scatter in the data presented in Figure 6 is caused by the lower probability of finding empty cavities in this mixture (i.e., the solute−solvent entropy drops) compared to acetone/water mixtures. Methane associates strongest with the DMSO methyl groups; however, unlike in acetone/water mixtures, water molecules occupy its first solvation shell to a significant extent as well. Integration over the first peak of the methane−water and methane−sulfur radial distribution functions (up to $R =$

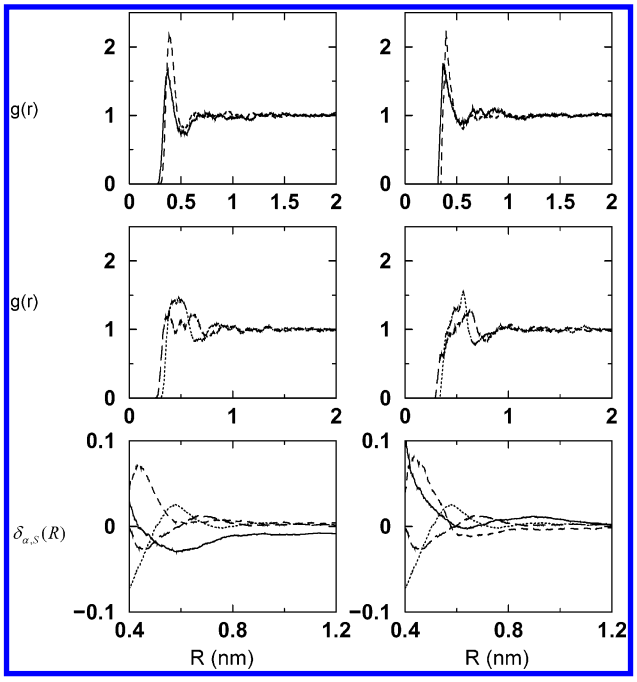

Figure 6. Methane−solvent radial distribution functions, $g(r)$, (upper two panels, left) and excess mole fractions, $\delta_{\alpha,S}(R)$, of solvent moieties α at distance R from the methane solute (lower panel, left) for solvent moieties water (solid line), methyl (dashed line), sulfur (dotted line), and sulfoxide oxygen (long dashed line) at a DMSO mole fraction of 0.48. The panels on the right show similar quantities for the cavity−solvent system.

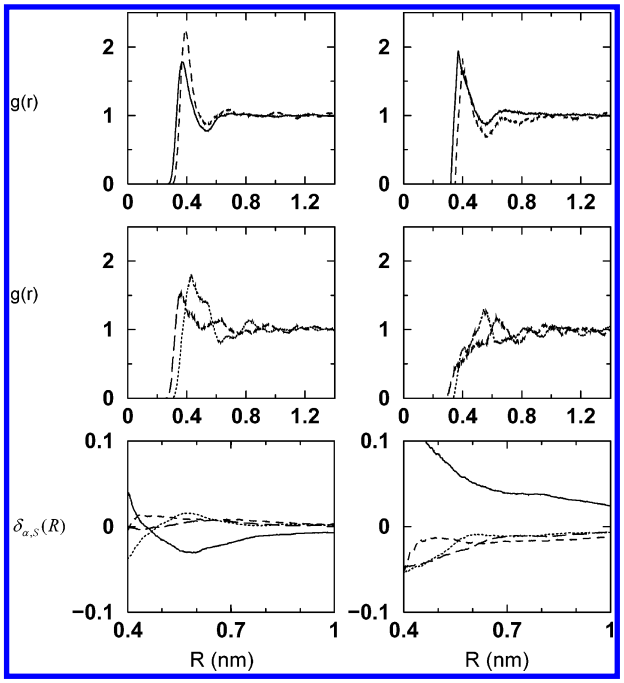

Figure 7. Methane−solvent radial distribution functions, $g(r)$, (upper two panels, left) and excess mole fractions, $\delta_{\alpha,S}(R)$, of solvent moieties α at distance R from the methane solute (lower panel, left) for solvent moieties water (solid line), methyl (dashed line), sulfur (dotted line), and sulfoxide oxygen (long dashed line) at a DMSO mole fraction of 0.10. The panels on the right show similar quantities for the cavity−solvent system.

0.65 nm) gives 7 hydration water molecules and 7.7 DMSO molecules. Hence, at this distance, the solvent/cosolvent distribution is almost random. At larger distances, a weak preferential solvation of methane by DMSO is observed in $\delta_{\alpha,S}(R)$ (lower left panel). The cavity−solvent and methane−solvent radial distribution functions are very similar. Cavities mainly contain DMSO methyl groups and water in their first solvation shells while the polar S═O moiety orients toward the bulk. At distances larger than 0.8 nm, a slight preference for water causes $\delta_{W,HS}(R)$ to lie slightly above $\delta_{DMSO,HS}(R)$. Because there is no strong preferential binding of either DMSO or water to the cavity, the slope in the solute−solvent entropy curve at $x_{DMSO} = 0.5$ becomes zero (Figure 5).

Methane and cavity solvation structures at a DMSO mole fraction of 0.10 are shown in Figure 7. At this composition, the solute−solvent entropy versus x_{DMSO} has a negative slope (Figure 5) and cavities are indeed preferentially hydrated (Figure 7, lower right panel). In contrast, methane is preferentially solvated by DMSO at distances larger than 0.5 nm (Figure 7, lower left panel). Methane, therefore, does not occupy cavities most likely to occur in the solvent (as in the case of acetone). Instead, it competes with water in associating with DMSO. This process, driven by the solute−solvent energy, is opposed by the entropy.

The weaker preferential binding of cosolvent molecules to methane in DMSO/water mixtures compared with that in acetone/water mixtures is caused by stronger hydration of the DMSO molecule compared to that of the acetone molecule. Because the DMSO/water mixture behaves like an ideal mixture in comparison to the acetone/water mixture (see above), in the former mixture solvent components may be viewed as being randomly mixed. Any preferential association of solvent components is likely correlated to preferential solute−solvent binding. A recent MD study of different urea models has indicated that preferential solvent binding to empty cavities in urea/water mixtures correlates with the extent of urea aggregation.[28]

5. Discussion

Solute−Solvent Entropy Changes versus Solvent−Solvent Interactions. We have shown how changes of the solute−solvent entropy with the cosolvent/water ratio are related to the nature of solvent−solvent interactions in the mixed solvent. In acetone/water mixtures, acetone−water interactions are weaker than those between water molecules in neat water. Added acetone preferentially binds to methane and favors methane solubility. This process is driven by a favorable change of the solute−solvent entropy. Opposite effects occur when sodium chloride is added to water. One may argue that binary solvents composed of mutually weakly (strongly) interacting components generally have a lower (higher) density than water (see Table 2) causing solute−solvent entropies to always rise (fall) relative to their values in pure water. Although the solute−solvent entropy sensitively depends on density, the above argument does not generally hold. To illustrate this, we performed a constant temperature (298.15 K) and pressure (1 atm) simulation of the 50/50 mole fraction acetone/water system (Table 2) replacing the acetone carbonyl oxygen and carbonyl carbon van der Waals C_{12} and C_6 parameters (Table 1) with the GROMOS96 parameters[38] while leaving all other parameters unchanged. The changed parameters are the following: $C_6^{1/2}(i,i) = 0.048\ 38$ [kJ/mol nm^6]$^{1/2}$, $C_{12}^{1/2}(i,i) = 1.837 \times 10^{-3}$ [kJ/mol nm^{12}]$^{1/2}$ (carbonyl carbon), $C_6^{1/2}(i,i) = 0.047\ 56$ [kJ/mol nm^6]$^{1/2}$, and $C_{12}^{1/2}(i,i) = 0.8611 \times 10^{-3}$ (1.125×10^{-3}) [kJ/mol nm^{12}]$^{1/2}$ (carbonyl oxygen). The C_{12} parameter in parentheses was used for carbonyl oxygen−water interactions. The SPC water model was used. With the GROMOS96 parameters the mixture assumes a density of 0.93 g/cm^3, which is 4% lower than the density of SPC water. The methane solute−solvent entropy,

however, does not rise but instead falls relative to its value in pure water, the reduction amounting to $T\Delta\Delta S^*_{uv} = -1.2$ kJ/mol. Inspection of the carbonyl-oxygen−water-oxygen radial distribution function showed a deeper minimum after the first peak indicative of stronger bound first shell hydration water.

This result has consequences for our notion of the solute−solvent entropy. Because it essentially is an excluded volume term the value of which is primarily determined by the solute's hard core size,[24] one would expect it to get stronger negative (opposing solubility) in denser liquids. Dense liquids may find fewer ways to configure small packets of free volume in order to open up a molecular-sized cavity, but this process must depend on the nature of the solvent molecules and the ways in which they mutually interact. It has been argued that liquids composed of small molecules (i.e., water) distribute their free volume in smaller packets than do organic liquids composed of larger molecules.[13−17] In the former case, the entropic cost to open up a cavity of a given size would be significantly larger, explaining the large entropy change opposing the solubility of hydrophobic solutes.[13] This view, however, has been criticized,[15,16] and it has been argued that the plasticity of water's hydrogen-bonded network suppresses its ability to open up molecular-sized cavities.[8] Not merely the small molecular size but also the molecular scale flexibility of the medium to configure its free volume plays a decisive role in aqueous solvents. We believe this latter view is crucial in rationalizing the observations we have presented in this paper. The weaker interaction of acetone with water compared to the interactions between water molecules themselves facilitates the process of opening up cavities close to acetone molecules in the mixed solvent. Much stronger bound hydration waters of cosolvents such as DMSO, the modified acetone above, and, in particular, sodium chloride suppress density fluctuations that open up cavities.

6. Conclusions

Molecular dynamics simulations were performed to study the hydration thermodynamics of methane infinitely diluted in binary cosolvent/water mixtures. The cosolvents sodium chloride (NaCl), dimethyl sulfoxide (DMSO), and acetone were studied at various cosolvent/water ratios and analyzed in terms of solute−solvent energy and entropy changes upon solute insertion. The "salting-in" and "salting-out" behavior of the cosolvents was analyzed in terms of the above two contributions to the solvation free energy as well as the liquid structure in the vicinity of the nonpolar solute. NaCl salts out methane as the result of an unfavorable solute−solvent entropy change. We find that this salting-out process is caused by strong intermolecular cosolvent−water interactions that impede the opening of cavities close to the cosolvent species causing the nonpolar solute to be preferentially hydrated. Acetone and DMSO salt in nonpolar solutes. Both cosolvents preferentially bind to the nonpolar solute, but the microscopic driving forces differ. Addition of acetone to water facilitates formation of empty molecular-sized cavities causing the salting-in process to be largely entropy driven. In addition, a favorable solute−solvent energy change reinforces the increase of the solute−solvent entropy. Cavities are found to open up close to the cosolvent (the methyl groups in particular) causing the preferential binding of the solute to acetone. In DMSO/water mixtures with water mole fractions larger than 0.5, cavities are preferentially hydrated for similar reasons as those found in case of NaCl. Preferential binding of the nonpolar solute to DMSO is driven by a strongly favorable change of the solute−solvent energy with increasing DMSO content while being opposed by the change of the solute−solvent entropy.

Acknowledgment. We thank Paul Smith for stimulating discussions and providing his acetone data.

References and Notes

(1) Kauzmann, W. *Adv. Protein Chem.* **1959**, *14*, 1.
(2) Tanford, C. *The Hydrophobic Effect: Formation of Micelles and Biological Membranes*; John Wiley & Sons: New York, 1973.
(3) Ben-Naim, A. *Hydrophobic Interactions*; Plenum: New York, 1980.
(4) Dill, K. *Biochemistry* **1990**, *29*, 7133.
(5) Blokzijl, W.; Engberts, J. B. F. N. *Angew. Chem., Int. Ed. Engl.* **1993**, *32*, 1545.
(6) Hummer, G.; Garde, S.; García, A. E.; Pratt, L. R. *Chem. Phys.* **2000**, *258*, 349.
(7) Southall, N. T.; Dill, K. A.; Haymet, A. D. J. *J. Phys. Chem. B* **2002**, *106*, 521.
(8) Pratt, L. R. *Annu. Rev. Phys. Chem.* **2002**, *53*, 409.
(9) Lum, K.; Chandler, D.; Weeks, J. D. *J. Phys. Chem. B* **1999**, *103*, 4570.
(10) Huang, D. M.; Chandler, D. *Proc. Natl. Acad. Sci. U.S.A.* **2000**, *97*, 8324.
(11) Hildebrand, J. H.; Prausnitz, J. M.; Scott, R. L. *Regular and Related Solutions: The Solubility of Gases, Liquids, and Solids*; Van Nostrand Reinhold: New York, 1970.
(12) Prausnitz, J. M.; Lichtenthaler, R. N.; Gomes de Azevedo, E. *Molecular Thermodynamics of Fluid Phase Equilibria*; Prentice Hall: Upper Saddle River, New Jersey, 1999.
(13) Lee, B. *Biopolymers* **1985**, *24*, 813.
(14) Lee, B. *Biopolymers* **1991**, *31*, 993.
(15) Pohorille, A.; Pratt, L. R. *J. Am. Chem. Soc.* **1990**, *112*, 5066.
(16) Pratt, L. R.; Pohorille, A. *Proc. Natl. Acad. Sci. U.S.A.* **1992**, *89*, 2995.
(17) Madan, B.; Lee, B. *Biophys. Chem.* **1994**, *51*, 279.
(18) Lazaridus, T. *Acc. Chem. Res.* **2001**, *34*, 931.
(19) Graziano, G.; Lee, B. *Biophys. Chem.* **2002**, *101*, 173.
(20) Timasheff, S. N. *Biochemistry* **1992**, *31*, 9857.
(21) Timasheff, S. N. *Adv. Protein Chem.* **1998**, *51*, 356.
(22) Schellman, J. A. *Biopolymers* **1994**, *34*, 1015.
(23) Yu, H.-A.; Karplus, M. *J. Chem. Phys.* **1988**, *89*, 2366.
(24) Guillot, B.; Guissani, Y. *J. Chem. Phys.* **1993**, *99*, 8075.
(25) Graziano, G. *Can. J. Chem.* **2002**, *80*, 401.
(26) Kirkwood, J. G.; Buff, F. P. *J. Chem. Phys.* **1951**, *19*, 774.
(27) Ben-Naim, A. *Statistical Thermodynamics for Chemists and Biochemists*; Plenum Press: New York, 1992.
(28) Weerasinghe, S.; Smith, P. E. *J. Chem. Phys.* **2003**, *118*, 5901.
(29) Weerasinghe, S.; Smith, P. E. *J. Chem. Phys.* **2003**, *118*, 10663.
(30) Collins, K. D. *Biophys. J.* **1997**, *72*, 65.
(31) Kalra, A.; Tugcu, N.; Cramer, S. M.; Garde, S. *J. Phys. Chem. B* **2001**, *105*, 6380.
(32) Matteoli, E.; Lepori, L. *J. Chem. Phys.* **1984**, *80*, 2856.
(33) Ben-Naim, A. *Solvation Thermodynamics*; Plenum Press: New York, 1987.
(34) Widom, B. *J. Chem. Phys.* **1963**, *39*, 2808.
(35) Gallicchio, E.; Kubo, M. M.; Levy, R. M. *J. Phys. Chem. B* **2000**, *104*, 6271.
(36) Gallicchio, E.; Kubo, M. M.; Levy, R. M. *J. Am. Chem. Soc.* **1998**, *120*, 4526.
(37) Levy, R. M.; Gallicchio, E. *Annu. Rev. Phys. Chem.* **1998**, *49*, 531.
(38) Van Gunsteren, W. F.; Billeter, S. R.; Eising, A. A.; Hünenberger, P. H.; Krüger, P.; Mark, A. E.; Scott, W. R. P.; Tironi, I. G. *Biomolecular Simulation: The GROMOS96 Manual and User Guide*; vdf Hochschulverslag: ETH Zürich, Switzerland, 1996.
(39) Geerke, D. P.; Oostenbrink, C.; Van der Vegt, N. F. A.; Van Gunsteren, W. F. *J. Phys. Chem. B*, in press.
(40) Schuler, L. D.; Daura, X.; Van Gunsteren, W. F. *J. Comput. Chem.* **2001**, *22*, 1205.
(41) Berendsen, H. J. C.; Grigera, J. R.; Straatsma, T. P. *J. Phys. Chem.* **1987**, *91*, 6269.
(42) Berendsen, H. J. C.; Postma, J. P. M.; Van Gunsteren, W. F.; Hermans, J. In *Intermolecular Forces*; Pullman, B., Ed.; Reidel: Dordrecht, 1981; pp 331−342.
(43) Berendsen, H. J. C.; Postma, J. P. M.; Van Gunsteren, W. F.; DiNola, A.; Haak, J. R. *J. Chem. Phys.* **1984**, *81*, 3684.
(44) Ryckaert, J.-P.; Ciccotti, G.; Berendsen, H. J. C. *J. Comput. Phys.* **1977**, *23*, 327.
(45) Ben Naim, A.; Marcus, J. *J. Chem. Phys.* **1984**, *81*, 2016.
(46) Rowlinson, J. S.; Swinton, F. L. *Liquids and Liquid Mixtures*, 3rd ed.; Butterworth: London, 1982.